Bathymetry of the Tonga Trench and Forearc: a map series

Dawn J. Wright[1], Sherman H. Bloomer[1], Christopher J. MacLeod[2], Brian Taylor[3] and Andrew M. Goodlife[3]

[1]*Department of Geosciences, Oregon State University, Corvallis, OR 97331-5506 USA;* [2]*Department of Earth Sciences, University of Wales, Cardiff CF1 3YE, UK;* [3]*Department of Geology & Geophysics, School of Ocean & Earth Science & Technology, University of Hawai'i, Honolulu, HI 96822 USA*

Abstract

Four new bathymetric maps of the Tonga Trench and forearc between 14 °S and 27 °S display the important morphologic and structural features of this dynamic convergent margin. The maps document a number of important geologic features of the margin. Major normal faults and fault lineaments on the Tonga platform can be traced along and across the upper trench slope. Numerous submarine canyons incised in the landward slope of the trench mark the pathways of sediment transport from the platform to mid- and lower-slope basins. Discontinuities in the trench axis and changes in the morphology of the landward slope can be clearly documented and may be associated with the passage and subduction of the Louisville Ridge and other structures on the subducting Pacific Plate. Changes in the morphology of the forearc as convergence changes from normal in the south to highly-oblique in the north are clearly documented. The bathymetric compilations, gridded at 500- and 200-m resolutions and extending along ~500 km of the landward trench slope and axis, provide complete coverage of the outer forearc from the latitude of the Louisville Ridge-Tonga Trench collision to the northern terminus of the Tonga Ridge. These maps should serve as a valuable reference for other sea-going programs in the region, particularly the Ocean Drilling Program (ODP) and the National Science Foundation MARGINS initiative.

Introduction

In recent years, large, regional-scale bathymetric maps published in *Marine Geophysical Researches* have focused on various portions of the global mid-ocean ridge (Purdy et al., 1990; Macdonald et al., 1992; Cochran et al., 1992; Scheirer et al., 1996; Keeton et al., 1997). Here we present a regional-scale map series of a convergent margin, consisting of four foldout maps (Maps 1–4, found at the back of this issue) of the Tonga Trench and forearc between 14 °S and 27 °S (Figure 1). These maps provide a number of insights into the geology and structure of an active intraoceanic forearc and trench, and serve as a companion and reference for the more detailed geological studies of this region appearing elsewhere (e.g., Clift et al., 1998; Kelman, 1998; Clift and MacLeod, 1999), as well as a valuable reference for other sea-going efforts, such as ODP drilling and marine geological/geophysical cruises under the auspices of the National Science Foundation's MARGINS initiative (Taylor et al., 1998). The bathymetric grids used to create these maps are available on the World Wide Web as binary Generic Mapping Tools (GMT; Wessel and Smith, 1995) grid files (see Appendix).

Bathymetric studies of the Tonga Trench and forearc have been important tools in interpretations of geological processes along this margin for four decade, beginning with Raitt et al. (1955). The morphology of the trench slopes has been used as: (1) part of the interpretations of basement and sedimentologic processes (Fisher and Engel, 1969; Bloomer and Fisher, 1987; Tappin, 1994; Clift et al., 1998); (2) inferences about the consequences of the subduction of the large, aseismic Louisville Ridge (e.g., Dupont and Herzer, 1985; Lonsdale, 1986; Ballance et al., 1989; Pelletier and Dupont, 1990); and (3) interpretations of the structural consequences of the change in relative plate motion at the northern end of the Tonga Trench (e.g., Hawkins and Natland, 1975; Wright, 1992; Millen and Hamburger, 1998). The maps presented here build on these types of studies, and provide the most complete bathymetric data to date for most of the landward slopes of the trench.

Most of the bathymetric data presented in this map series were collected during Boomerang Leg 8 aboard
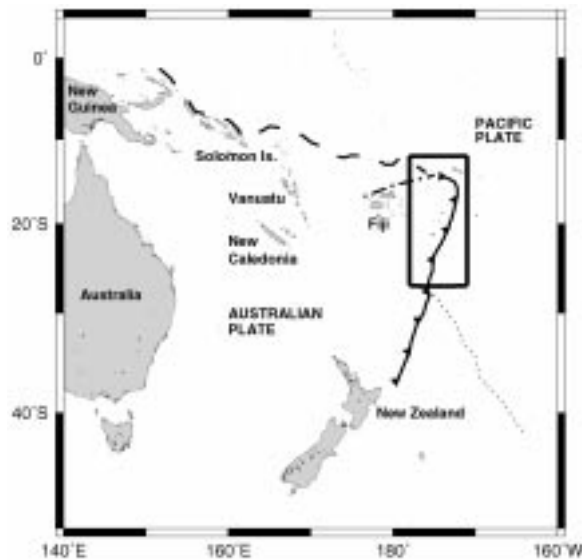
Figure 1. Regional location map of the study area (marked by box) in the southwest Pacific. Tonga Trench marked by solid line with barbs on overriding plate. Dashed line represents the trend of the Vitiaz Trench lineament (Brocher, 1985), and dotted-dashed line shows trend of the Fiji Fracture Zone (Kroenke et al., 1987). Trend of Louisville Ridge (Lonsdale, 1988) marked by dotted line.

R/V *Melville* (May to June 1996) using the Sea Beam 2000 multibeam swath mapping system (Figures 2 and 3). In addition to the bathymetry, Sea Beam 2000 sidescan, dual-channel seismic reflection data, Bell BGM-3 gravity, total field magnetics, and an extensive suite of dredged samples were collected. Sea Beam 2000 sidescan and seismic reflection data are presented elsewhere (Bloomer and Wright, 1996; Clift et al., 1998). Boomerang 8 was an ODP site survey and addressed a number of scientific issues concerning the origin and structure of the Tonga forearc. Chief among them were: (1) testing the hypothesis that the Tonga forearc is comprised of an ophiolitic basement (such as that exposed in Cyprus), formed in the earliest stages of subduction by high-volume, short-lived arc volcanism (Bloomer et al., 1996; Kelman, 1998); and (2) constraining the mechanisms of tectonic (subduction) erosion (i.e., the process by which material from the overriding plate is removed piecemeal and recycled into the mantle; Hussong and Uyeda, 1981; Hilde, 1983; Bloomer and Fisher, 1987), and how its effects may be distinguished from the subduction of the Louisville Ridge.

Geologic setting

Intraoceanic convergent margins are important sites of nascent continental crust formation and recycling of material back into the mantle. Here mantle-derived melts are transferred to the arc, forearc, and backarc system, and oceanic sediments and fragments of oceanic crust are accreted (Hawkins, 1974, 1995). Tonga is recognized as the type example of an extension-dominated, non-accretionary convergent margin (e.g., Tappin, 1994; Tappin et al., 1994a; MacLeod, 1996), with active extensional tectonism throughout the forearc and landward trench slopes.

The Tonga Trench is the site of westward subduction of the Pacific Plate beneath the northeastern corner of the Australian Plate (Figure 1). Relative plate convergence is at ~290° and is orthogonal to the 020° average trend of the trench (DeMets et al., 1990). The estimated convergence rate is approximately 15 cm/yr (Lonsdale, 1986); however, recent GPS measurements indicate an instantaneous convergence of 24 cm/yr across the northern Tonga Trench, which is the fastest plate velocity yet recorded on the planet (Bevis et al., 1995). At the northern terminus of the trench, near 15 °S (Map 1 at back), plate convergence gives way to complex strike-slip motion associated with the Fiji Fracture Zone and back-arc extension in the northern Lau Basin (Kroenke et al., 1987; Hamburger and Isacks, 1988; Millen and Hamburger, 1998). Along its southern end, at approximately 26 °S, the trench is impinged upon by the Louisville Ridge, a NNW-trending chain of hotspot-related guyots and seamounts on the Pacific Plate (Figure 1; Clague and Jarrard, 1973; Dupont and Herzer, 1985; Gnibdenko et al., 1985; Lonsdale, 1986, 1988; Watts et al., 1988), which may be traced for several hundred kilometers to the southeast, roughly paralleling the trend of the Hawaiian-Emperor Seamount chain (Clague and Jarrard, 1973). Because of the obliquity between the trend of the Louisville Ridge and the convergence direction of the Tonga Trench, the collision zone is migrating southward along the trench at a rate of approximately 18 cm yr^{-1} (Lonsdale, 1986; MacLeod, 1994). This rate is roughly equivalent to the rate of southward propagation of the Eastern Lau Spreading Center/Valu Fa Ridge within the Lau Basin (Parson and Hawkins, 1994). The visible effects of collision upon the trench are well seen near 26 °S, which also marks the boundary between the Tonga and Kermadec forearcs. In the vicinity of the collision zone near 26 °S, the trench axis is unusually shallow, with a max-

imum depth of less than 6000 m (Dupont and Herzer, 1985; Pontoise et al., 1986; Map 4 at back). To the north, the post-collisional trench axis is deeper and the inner trench slope is much narrower and far steeper (with slopes of 3–10° at 6000–9000 m depth; Maps 3 and 4 at back) than in the trench to the south of the intersection, where slopes average 1–2° and the maximum depth of the trench axis is typically 8000 m (Lonsdale, 1986). The axis of the Tonga Trench is off-set roughly 50 km to the northwest, relative to the axis of the Kermadec Trench (Figure 1). That offset has been attributed to erosion of the Tonga forearc induced by the subduction of the Louisville Ridge (Pelletier and Dupont, 1990).

Active arc volcanism is occurring along the Tofua volcanic arc (TVA), located on the western edge of the shallow forearc platform of the Tonga Ridge (Figures 2 and 3). The Tonga Ridge is part of a remnant arc complex, split in the late Miocene to form the active Lau backarc basin (Karig, 1970; Parson et al., 1992; Figures 2 and 3). The very broad, shallow form of the Tonga Ridge is very different from the western part of the Kermadec forearc (Pelletier and Dupont, 1990). The uplift of this platform has been attributed to the effect of the southward propagating subduction of the Louisville Ridge (Pelletier and Dupont, 1990), but it could also be a consequence of the original geometry of remnant arc rifting (Hawkins et al., 1984). The other half of the remnant arc, the Lau Ridge, forms the west-ern margin of the actively-spreading Lau Basin. The Lau Basin has a triangular shape as a consequence of the clockwise rotation of the Tonga Ridge as the basin opened (MacLeod et al., 1992, 1994; Sager et al., 1994; Olbertz et al., 1997).

The Tonga forearc lies between the TVA and the trench, including the Tonga platform, and comprises basement that appears to be wholly Eocene or younger in age (Bloomer et al., 1994). This volcanic base-ment is overlain by a sedimentary sequence comprised mainly of volcaniclastic sediments laid down during at least three episodes of arc volcanism (Hawkins et al., 1994). The still-active TVA represents the most recent episode. The forearc from 14 °S to 26 °S may be sub-divided latitudinally into three major blocks, based on morphology, structure, and sediment geometry (Tappin, 1994):

1. the northern block (north of ∼18°30′S; Maps 1 and 2 at back) lies in the deepest water, and includes small islands formed by TVA volcanoes that pene-trate a relatively thin sedimentary section with no preferential regional dip;

2. the central block (∼18°30′ to 22 °S; Maps 2 and 3 at back) is composed of numerous small islands with a sedimentary section dipping mainly towards the east, and the TVA lying on the western margin of this part of the forearc; and

3. the southern block (∼22° to 26 °S; Maps 3 and 4 at back) is entirely submarine with shallow water depths, a sedimentary section dipping westward towards the Lau Basin, and the TVA against the western margin of the forearc.

GPS-derived plate convergence vectors between the Tonga platform and the Pacific plate suggest that the forearc is rapidly rotating clockwise at a rate of ∼7° Myr^{-1} (Bevis et al., 1995). This is in accord with paleomagnetic data from ODP sites on the Tonga forearc and from field studies on the islands, indicat-ing 20° of clockwise rotation since the late Miocene (MacLeod et al., 1992; Sager et al., 1994).

Data acquisition

The Sea Beam 2000 bathymetric mapping system operates at 12 kHz with 121 across-track beams (com-pared to 16 for Sea Beam), yielding a swath roughly 3.46 times the water depth (Miller and Capell, 1993). The beams are automatically adjusted to be equidistant horizontally. The data were logged into time series and archived into files containing 24 hours worth of data. Files were then run through scripts that merged them with 24-hour P-code Global Positioning Sys-tem (GPS) navigation. Track charts and speed/course consistency used in the Eotvos corrections for gravity anomaly calculations showed the P-code navigation to be significantly better than S-code. GPS data aboard the *Melville* were collected with PCODE and Trimble 4000AX receivers. Any navigational errors resulting from a temporary malfunction of the PCODE GPS were replaced with fixes from the Trimble 4000AX. For the majority of the 36-day cruise the PCODE re-ceiver performed flawlessly, with no editing of the navigation needed.

Sound velocity profiles were taken every 2.5 days during the cruise, for a total of fourteen. Expendable bathythermographs (XBTs) deployed every few days verified that the profiles remained within acceptable limits. Very small spatial variations in sound speed

matched well with those in the temporal domain, so the profiles that were used to calculate depths were not altered.

It should be noted that the tracklines of Boomerang 8 were not planned exclusively for a mapping program (Figures 2 and 3). The dredging and seismic programs of Boomerang 8 were also extremely important, as they were essential for understanding the origin, composition, and structure of the Tonga forearc. On the basis of beam coverage alone it would have been more efficient to run our survey lines, for the most part, parallel to the axis of the forearc and trench, with a few perpendicular lines across major off-axis features such as the Capricorn seamount. But given the importance of the other programs, the mixture of perpendicular and parallel tracks was the best choice, still providing nearly complete coverage of the outer forearc and the north- and southeast limbs of the King's Triple Junction at 174 °W (Figure 2). The Boomerang 8 Sea Beam 2000 data combined with Sea Beam 2000 data from Westward Legs 5, 6, and 12 (Smith et al., 1998), provide complete coverage of Capricorn seamount and one swath on the Pacific plate parallel to the trench axis (Figures 2 and 3; Table 1). The inclusion of Sea Beam data from Marathon 6 (Lonsdale, 1986; Table 1), consisting of one swath running down the trench axis throughout the study area, the R/V *Sonne* cruises SO-35, SO-48, and SO-67 (Beiersdorf and von Stackelberg, 1990; von Stackelberg and von Rad, 1990; von Rad et al., 1990; Table 1), and center beam depths from the R/V *Jean Charcot* cruises JC-86000211 and JC-87001211 (used to supplement the multibeam coverage from 23°–27 °S; Table 1), as well as an edited compilation of digitized contours from New Zealand hydrographic charts (New Zealand Hydrographic Office, 1997), yields nearly complete coverage for the entire study area.

Data processing

Data processing was accomplished using MB-System (Caress and Chayes, 1996; Caress et al., 1996), and additional code written by D. Scheirer and the Scripps Institution of Oceanography (SIO) Shipboard Computer Group. GMT was used for shipboard display and plotting, as well as for preparation of the final map series. Time series of bathymetry data were initially merged with the logged navigation and then run through a program that unflagged beams automatically flagged as bad by Sea Beam Instruments software. We

found that the software often flagged 8–10% of the good beams for deletion, particularly in the deep terrain of the Tonga Trench. The data were then passed through a despiking algorithm that filtered the unflagged data. Care was taken to remove ping data acquired at a ship's speed of less than 4 knots over dredging sites. All data were then edited manually using mbedit, MB-System's visually interactive, ping-editing tool. This tool allows the user to cycle through each ping in the data set and remove bad beams that may have been missed during the filtering step. The data were of high enough quality that we were able to keep the editing abreast of the data collection rate. The small number of artifacts included the occasional 'curling up' of outermost beams, 'loss of bottom' on very steep slopes, and spurious depth readings resulting from sudden heading changes (greater than 10°/min) in deep terrain during dredging operations.

The final bathymetry grids were constructed by combining gridded data from all of the individual surveys, giving priority to the more recent surveys with Sea Beam 2000. Raw, ping-edited Sea Beam 2000 data files were readily available while the Sea Beam data from R/V *Sonne* cruises had already been gridded, and therefore had to be resampled, edited, and regridded. Gridding was based on a Gaussian weighted average scheme. Each data point's contribution to a Gaussian weighted average for each nearby grid cell was calculated as the point was read and added to the grid cell sums (Caress and Chayes, 1995). A weighted average scheme was chosen because in the absence of artifacts, it does the best job of representing the gridded field. Also, the scheme is heavily biased towards those data points closest to the grid point and minimizes anomalous values from outliers (Keeton et al., 1997). Gaps between swaths were filled using a thin plate spline (i.e., a common smoothing function; see Sandwell, 1987) with a tension of infinity. The size of the internal working grid was increased up to of 0.1 times the size of the grid to guide the spline interpolation of data gaps, which may have occurred at the edges of the grid. The clipping dimension for the spline interpolation was increased by varying distances, up to 10 times the grid spacing, in order to fill data gaps. For high resolution grids of small areas (thin boxes in Figures 2 and 3), a grid spacing of 200 m was chosen as this matches the footprint of each Sea Beam 2000 beam at ∼5000–6000 m depth. Larger, regional grids (thick boxes in Figures 2 and 3) were gridded at 500 m.

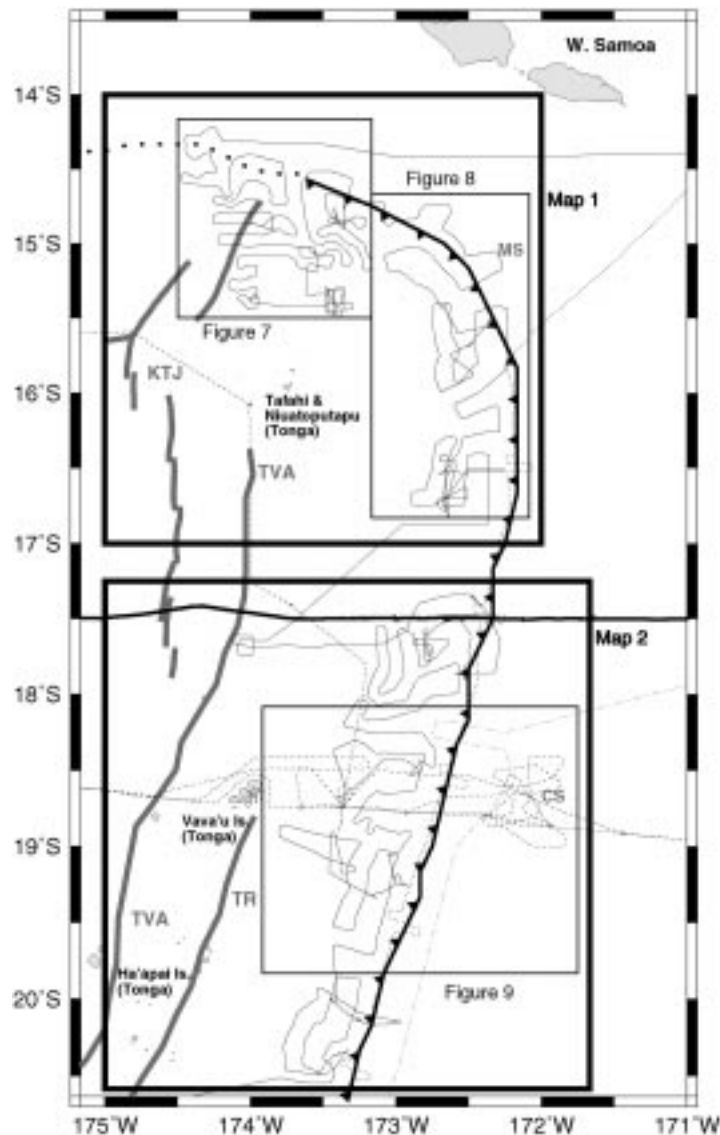Detailed bathymetry of the Tonga platform, as digitized from New Zealand hydrographic charts (New

Figure 2. Index map showing major tectonic features and ship tracks of data used for the northern half of the map series. Tonga Trench marked by thick solid line with barbs on overriding plate, and Fiji Fracture Zone by thick dotted line. Heavy lines = King's Triple Junction (KTJ; also known as the Mangatolu Triple Junction), axis of nascent spreading center, axis of Tofua volcanic arc (TVA), axis of Tonga Ridge (TR). Also shown are locations of Machias seamount (MS), and Capricorn seamount (CS). Thin solid line = tracks of Boomerang Leg 8; thick solid line at 17°30′ S = Westward Leg 5; dashed line = Westward Leg 6; dotted-dashed line = Westward Leg 12; thin dotted line = Marathon 6. Thick solid boxes indicate areas of the large regional maps at the back of this issue (made primarily from 500-m Sea Beam and Sea Beam 2000 grids). Thin solid boxes indicate areas and figure numbers of the more detailed, higher resolution maps that appear in the manuscript (made from 200-m Sea Beam 2000 grids).

Zealand Hydrographic Office, 1997), was block-median filtered before merging with the Sea Beam data. Additional data editing control over this region and in certain areas along the trench axis was obtained by masking selected small areas and interpolating over them between good data points with a pure spline solution. In practice, gaps smaller than 3 km were filled in. Center-beam depths from the *Jean Charcot* cruises at 23°–27 °S were manually edited to remove large artifacts and then block-median filtered before merging with Sea Beam data.
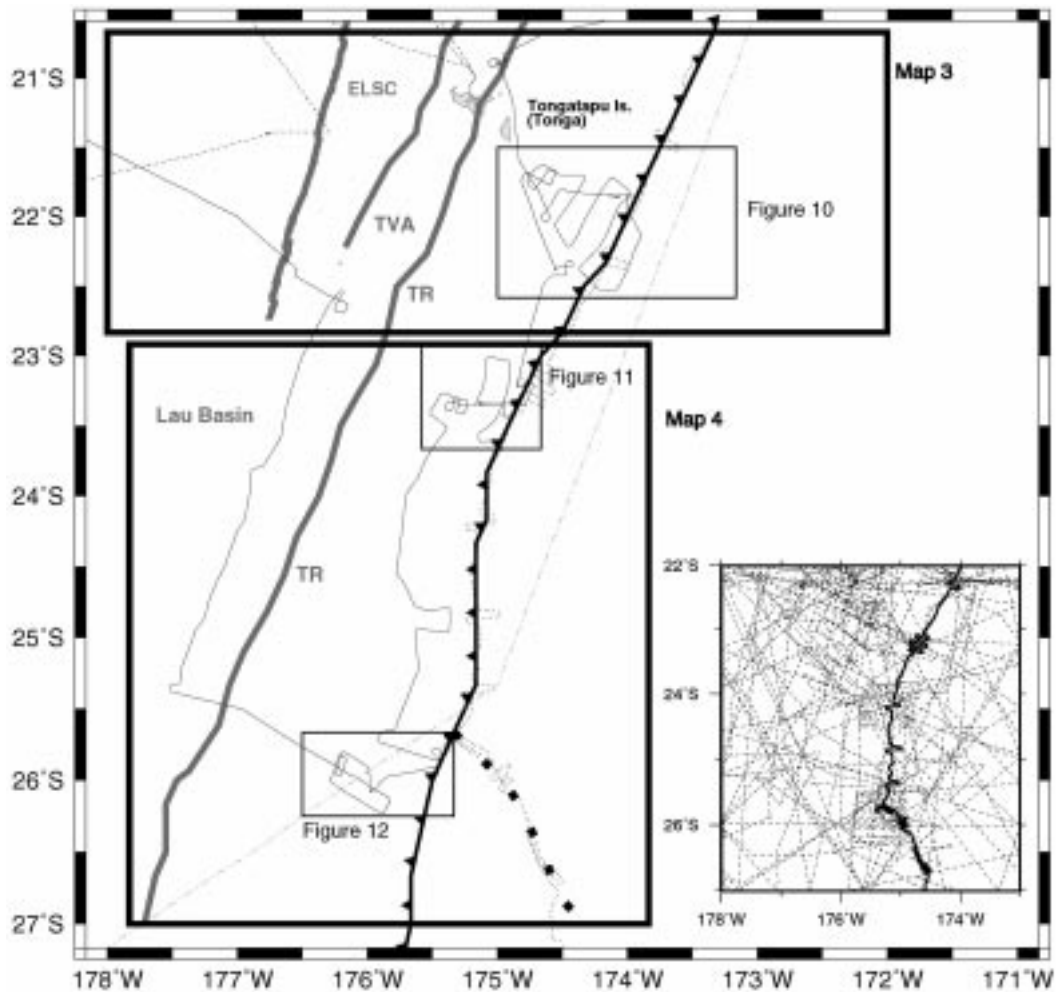
Figure 3. Index map showing major tectonic features and ship tracks of data used for the southern half of the map series. Tonga Trench marked by thick solid line with barbs on overriding plate. Heavy solid lines = Eastern Lau spreading center (ELSC) within the Lau Basin, axis of Tofua volcanic arc (TVA), and axis of Tonga Ridge (TR). Heavy dashed line = axis of Louisville Ridge. Thin solid line = tracks of Boomerang Leg 8; dashed line = Westward Leg 6; dotted-dashed line = Westward Leg 12; dotted line = Marathon 6. Inset map shows tracks of Marathon 6 down the trench axis (heavy line) with cruises of the R/V *Jean Charcot* (dashed lines; see Table 1). Thick solid boxes indicate areas of the large regional maps at the back of this issue (made primarily from 500-m Sea Beam and Sea Beam 2000 grids). Thin solid boxes indicate areas and figure numbers of the more detailed, higher resolution maps that appear in the manuscript (made primarily from 200-m Sea Beam 2000 grids).

The maps

The map series consists of four foldout maps at the back of this issue. Each is plotted at a Mercator projection using the WGS 84 spheroid. The scales of each map, optimized for the published format size are: Map 1 = 1:500,000, Map 2 = 1:560,000, Map 3 = 1:700,000, and Map 4 = 1:670,000. The colors for each of the maps correspond to the same depth interval (500 m), and the contour interval is 250 m. Maps 1–3 are based on a 500-m gridded data set, while Map 4 is based on a data set primarily of center-beam soundings, gridded at 30 seconds. Even though we endeavored to remove all of the bathymetry artifacts, a number of small ones remain, particularly at the transitions between GPS-navigated Sea Beam 2000 and Transit satellite-navigated Sea Beam surveys (e.g., upper right corner of Map 2). The quality of navigation of the Sea Beam surveys is variable, with an estimated navigational accuracy of ±250–300 m (Beiersdorf and von Stackelberg, 1990; Wiedicke and Collier, 1993; Wiedicke and Habler, 1993). Depths shown on all maps are in corrected meters.

Table I. Swath data sources

Cruise	Dates	Ship	Principle Objectives	Multibeam System	PI(s)
Boomerang 8	May–June 1996	*Melville*	ODP site survey: multibeam, dredging, seismics	Sea Beam 2000	Bloomer, Wright
Westward 12	April–May 1995	*Melville*	transit	Sea Beam 2000	–
Westward 6	Aug.–Sep. 1994	*Melville*	OBS, seismic, multibeam	Sea Beam 2000	Hildebrand, Dorman
Westward 5	May–June 1994	*Melville*	OBS, multibeam	Sea Beam 2000	Bryden
SO-67	Feb. 1990	*Sonne*	multibeam	Sea Beam	Wiedicke, Collier, Habler
SO-48	Feb. 1987	*Sonne*	multibeam	Sea Beam	Riech, von Stackelberg, von Rad
SO-35	Dec. 1984– Jan 1985	*Sonne*	multibeam	Sea Beam	von Stackelberg, von Rad
Marathon 6	Aug.–Sep. 1984	*Thomas Washington*	multibeam, seismics	Sea Beam	Lonsdale
JC-87001211	Mar.–Apr. 1987	*Jean Charcot*	bathy, magnetics, gravity	Sea Beam (only center beam depths available)	–
JC-86000211	Jan. 1986	*Jean Charcot*	bathy, magnetics, gravity	Sea Beam (only enter beam depths available)	–

Discussion of bathymetric features

Here we simply summarize the primary morphological features that can be seen in the maps, starting from the northwest corner of the study area, moving east around the 'corner' of the Tonga Trench and then south. More detailed geological interpretation and analysis of these data will be presented elsewhere, in conjunction with seismic, sidescan, and geochemical data. Figure 4 shows the location of a series of profiles generated from Sea Beam 2000 center beam depths and projected perpendicular to the trend of the trench and forearc. The profiles were selected both to show a regional overview of the trench and forearc, where the best Sea Beam 2000 data were available, and to be representative of the typical morphology of an extension-dominated convergent margin. Profiles 1–18 (Figures 4 and 5) cover the northern terminus of the trench, the axis of seafloor-spreading in the northeast limb of the King's Triple Junction, and the northern forearc block. Profiles 19–23 are representative of the central forearc block, and profiles 24–30 are from the southern forearc block (Figures 4 and 6).

A primary hypothesis guiding the discussion of bathymetric features is that vigorous tectonic erosion of the Tonga forearc is occurring at the present time (based on results from ODP Leg 135; MacLeod, 1994; Clift and MacLeod, 1999). It is also thought that erosion may be occurring by a combination of two distinct mechanisms: (1) a spatially restricted process resulting from subduction of the Louisville Ridge, and (2) a quasi-steady-state 'background' mechanism occurring everywhere along the trench and forearc. While bathymetry can provide surficial evidence of tectonic erosion, insights into the mechanisms and causes of the process require drilling, in order to investigate the magnitude and timing of subsidence across the forearc, as well as the detailed structure of the forearc basement.

Regional features

The four maps clearly show the broad, shallow Tonga platform at the east end of the forearc. Broad, isolated highs that are extensions of this uplifted, old, arc basement can be found as far north as 15°30′ S, though the expression of the Platform is greatly subdued north
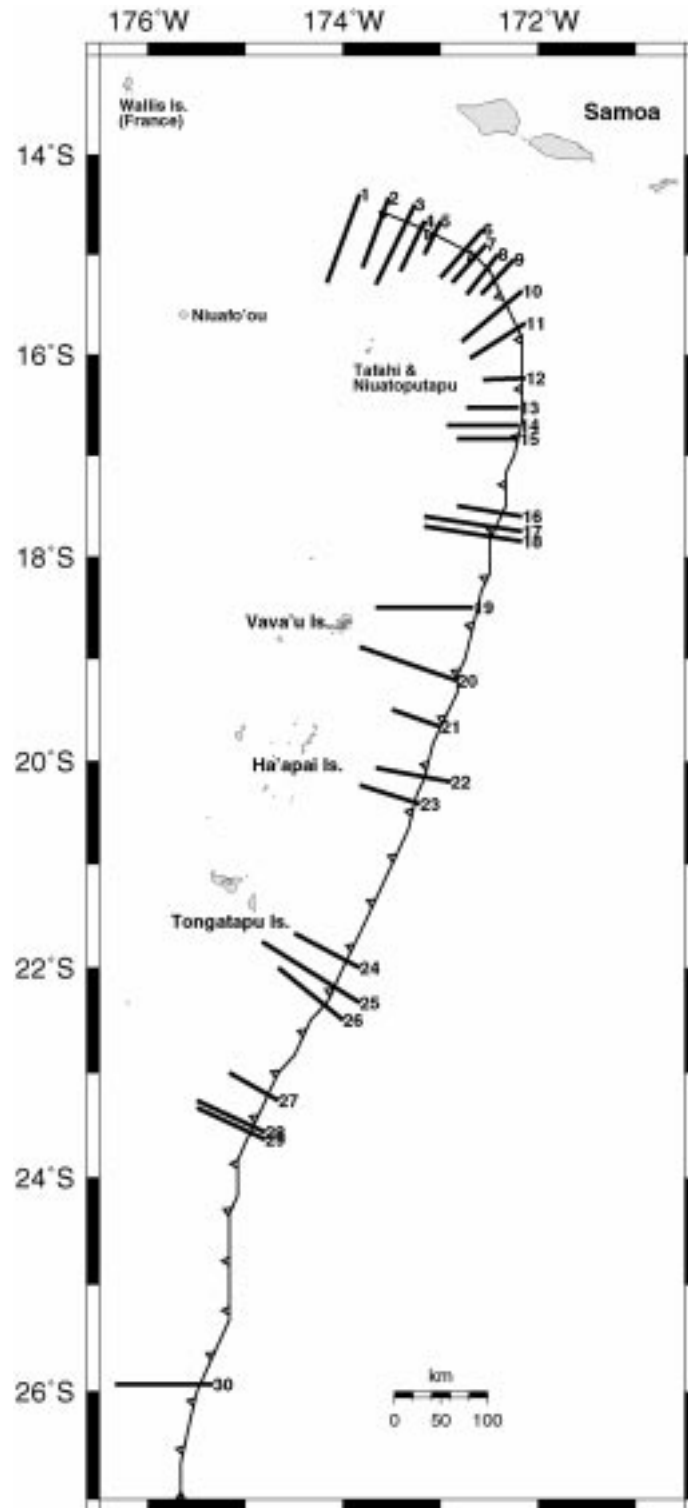
496

Figure 4. Index map of selected bathymetric profiles across the Tonga Trench and forearc.
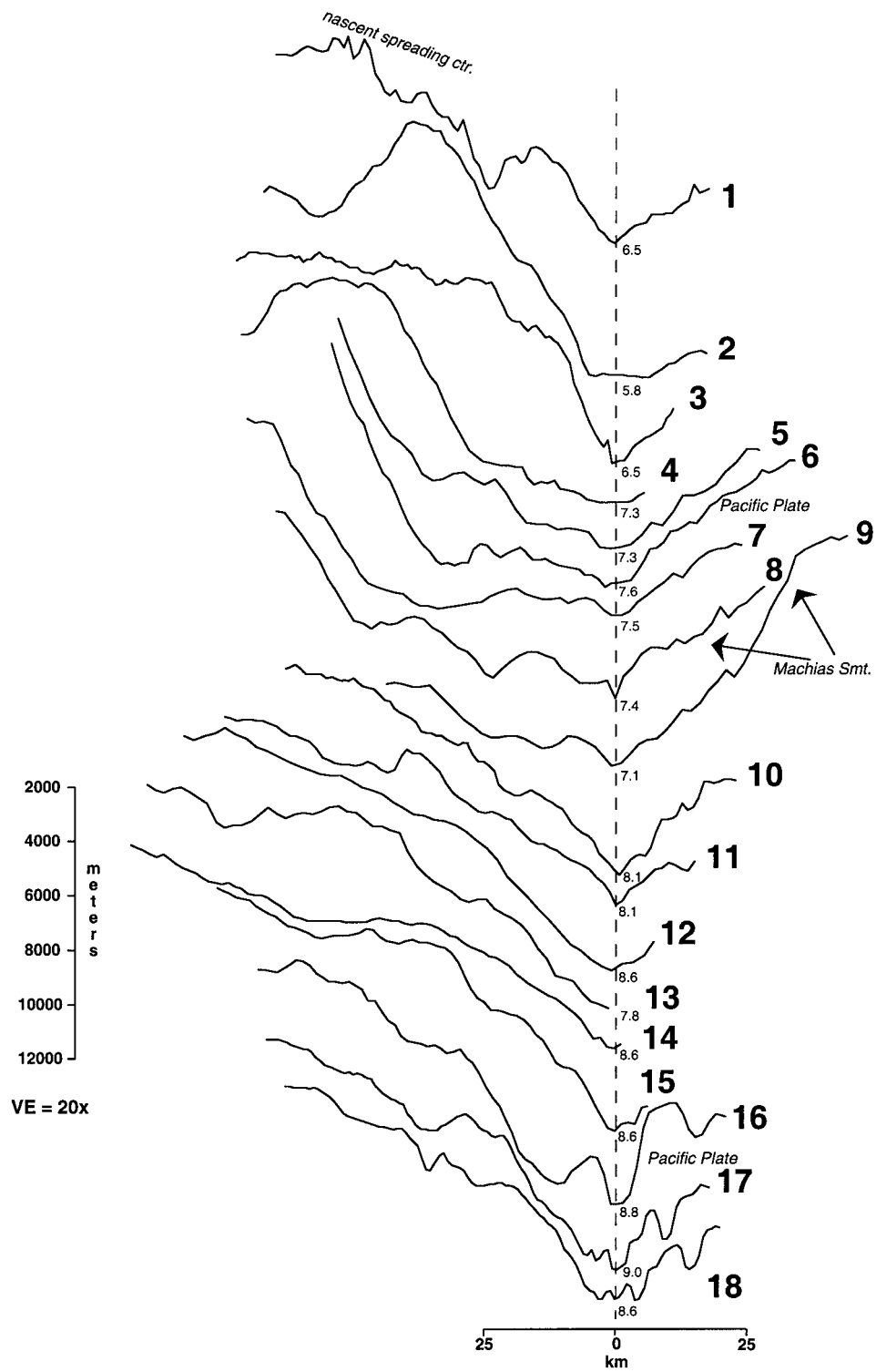
Figure 5. Bathymetric profiles across the northern Tonga Trench and forearc. Profiles are from the center beam of Sea Beam 2000 swaths and have been projected normal to the trench axis. Dashed line shows location of trench axis, and small numbers at bottom of each profile denote maximum depths in kilometers.
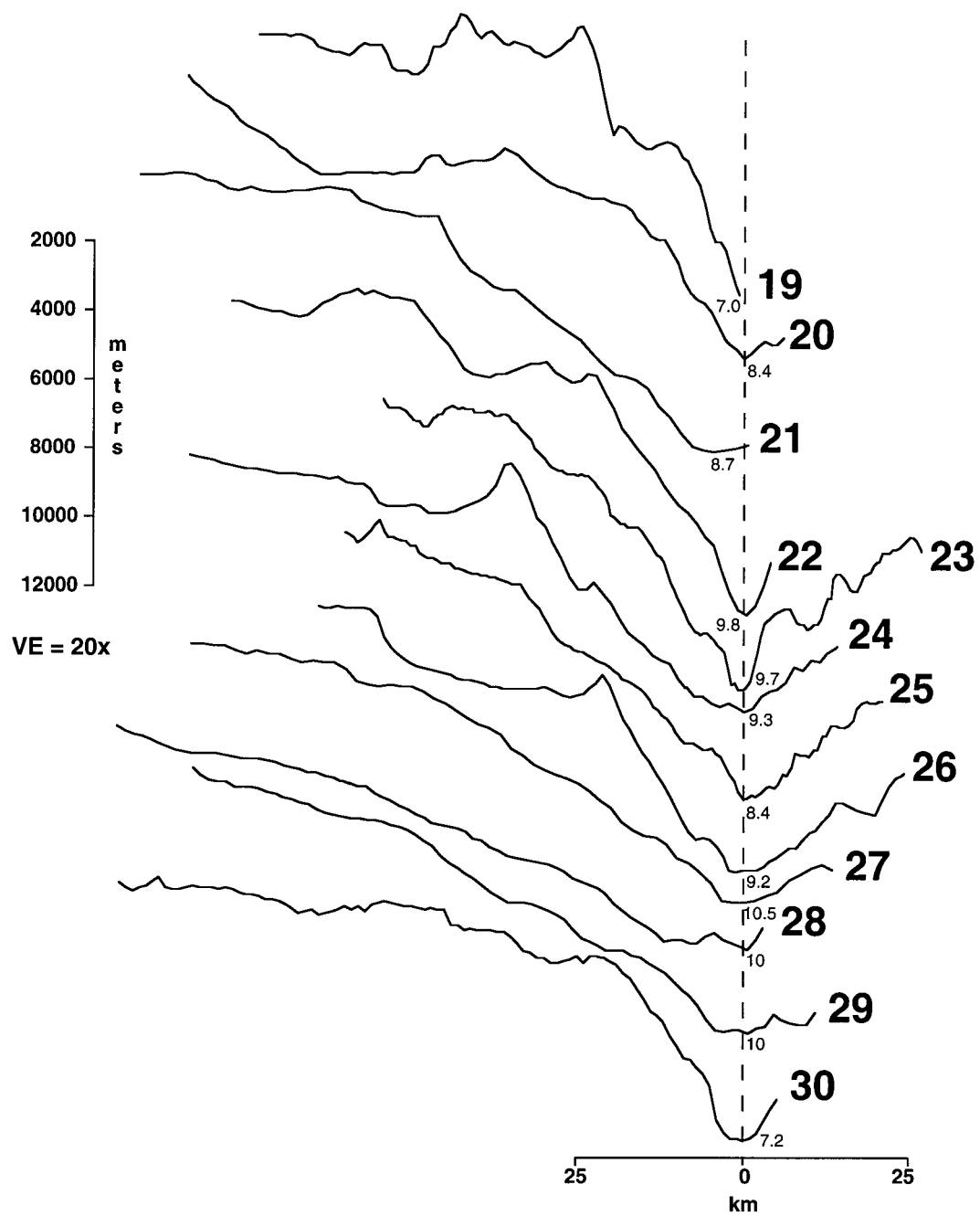
498

Figure 6. Bathymetric profiles across the central and southern Tonga Trench and forearc. Profiles are from the center beam of Sea Beam 2000 swaths and have been projected normal to the trench axis. Dashed line shows location of trench axis, and small numbers at bottom of each profile denote maximum depths in kilometers.

of 18°30′ S. The forearc deepens dramatically off the eastern edge of the platform, and generally has very steep, narrow landward slopes.

All of the maps show evidence of irregular highs along the trench-slope break and in the mid- and lower-trench slopes. These blocks are commonly asymmetric and all of them that were sampled yielded altered volcanic basement and volcaniclastic sediments (Bloomer et al., 1996). These highs appear to be structural blocks, bounded by normal faults, and are not cored by serpentinites as are many of the trench-slope highs in the Izu-Mariana-Bonin trench (e.g., Fryer et al., 1985, 1990). The maps identify major canyons that provide pathways for material to be transported from the central and eastern Tonga Platform to the trench axis and mid- to lower-slope basins.

The maps show consistent changes in the morphology of the forearc and trench as convergence changes from highly oblique to normal in the north and as the time since collision of the trench with the Louisville Ridge increases. We look briefly at some of those changes in the next four sections.

Map 1: A strike-slip boundary and the termination of the Trench

Map 1 (at back) includes the most tectonically complex terrain of the entire study area, including the transition from subduction to strike-slip motion, and the north- and southeast limbs of the King's Triple Junction (also known as the Mangatolu Triple Junction; Hawkins, 1986; Hawkins et al., 1994; Taylor et al., 1996). The northernmost edifices of the TVA (14°57′ S, 173°27′ W) extend to within 40 km of the trench axis. Volcanic cross-chains in the active arc can be identified at 15°05′ S, 174°40′ W; 15°20′ S, 173°40′ W; and 16°20′ S, 173°50′ W.

Figure 7 shows a map view of a nascent spreading center, featuring a series of parallel, closely-spaced ridges and troughs, a morphology reminiscent of that observed at slow-spreading ridges. The spreading center can be clearly identified to within about 30 km of the trench axis, and may extend farther north than that. Its juncture with the trench presumably forms a ridge-transform-transform boundary between the Tonga forearc, the Pacific plate, and the Australian plate. Almost directly to the south of this fabric lies a 10-km wide caldera with a significant breach on its southern rim. The caldera lies slightly west of the main line of TVA volcanoes. Dredges from the caldera yielded dacite lavas, which may de-

rive from both the adjacent TVA and the back-arc spreading center (Bloomer and Wright, 1996). The spreading fabric and the caldera probably result from coupling between the crust of the Tonga microplate and the tearing, subducting Pacific plate, accompanied by lateral southward flow of asthenospheric mantle (MacLeod, 1996). This is supported by the geochemistry of lavas from northern Tonga (Falloon et al., submitted). The spreading fabric lies roughly parallel and to the east of the northeastern limb of the King's Triple Junction, a back-arc ridge-ridge-ridge triple junction that is developing within rifted arc crust (Figure 2). The core of the King's Triple Junction is located at approximately 15°37′ S, 174°52′ W, and is characterized by intense deformation and neovolcanism (Parson and Tiffin, 1993). The Boomerang 8 Sea Beam 2000 survey covered its northeast limb, centered at ~174°00′ W and trending NE at ~025° for a distance of ~50 km (Map 1 at back), as well as its lengthiest limb, extending over 200 km south from 15°37′ S to 17°40′ S (Maps 1 and 2 at back). Future geochemical analyses will be required to determine what, if any, connection exists between the northeastern limb of the King's Triple Junction and the nascent spreading center that parallels it.

To the west of the nascent spreading center (Figure 8, Map 1), the trench shoals rapidly and the southern slope lacks any obvious lineations. The southern slope is very steep, and has large mid- and upper-slope highs (Profiles 1 and 2). This region likely links the Tonga Trench to the seismically defined Fiji Fracture Zone (Millen and Hamburger, 1998), but the nature or precise location of this plate boundary is not at all clear. Seismicity distributions (e.g., Hamburger and Isacks, 1988) require that the boundary be a broad (~100 km) transfer zone, rather than a simple transform fault.

Part of Profile 1 is located along the axis of the nascent spreading center. To the southeast, the trench axis becomes broad and relatively flat (Figure 5; Profiles 4–9), with more symmetrical landward and seaward slopes, as first noted by Raitt et al. (1955). This portion of the trench (from about 14°40′ S, 173°30′ W to 15°10′ S, 172°30′ S) marks a zone either of strike-slip motion between the forearc and the Pacific Plate, based upon an inferred convergence direction of about 110° (Pelletier and Louat, 1989), or oblique slip as inferred by Millen and Hamburger (1998).

The tearing of the Pacific plate at the northern terminus of the Tonga Trench (Figure 8) was first proposed by Isacks et al. (1968), with solid supporting
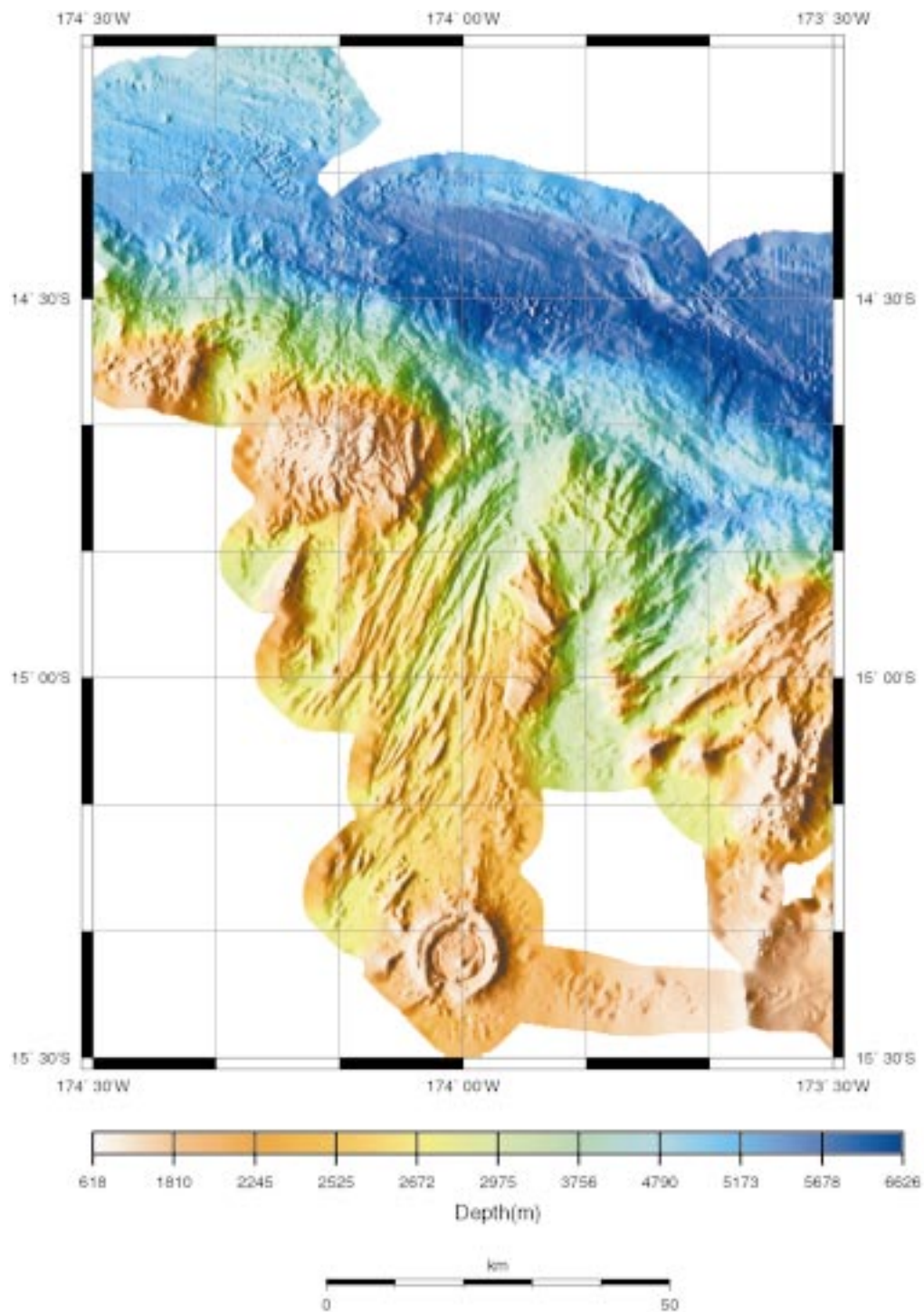
Figure 7. Histogram equalized, shaded relief bathymetric map, created from a 200-m Sea Beam 2000 grid (Boomerang 8), of a small ridge-transform-transform boundary to the west of the Tonga Trench. The bathymetry is illuminated at an azimuth of 90° using a shading magnitude of 0.4 to accentuate the spreading fabric of the ridge centered at 174 °W, as well as a back-arc caldera at ~15°25′ S, 174 °W. Color change interval based on histogram equalization. Map projection is Mercator.
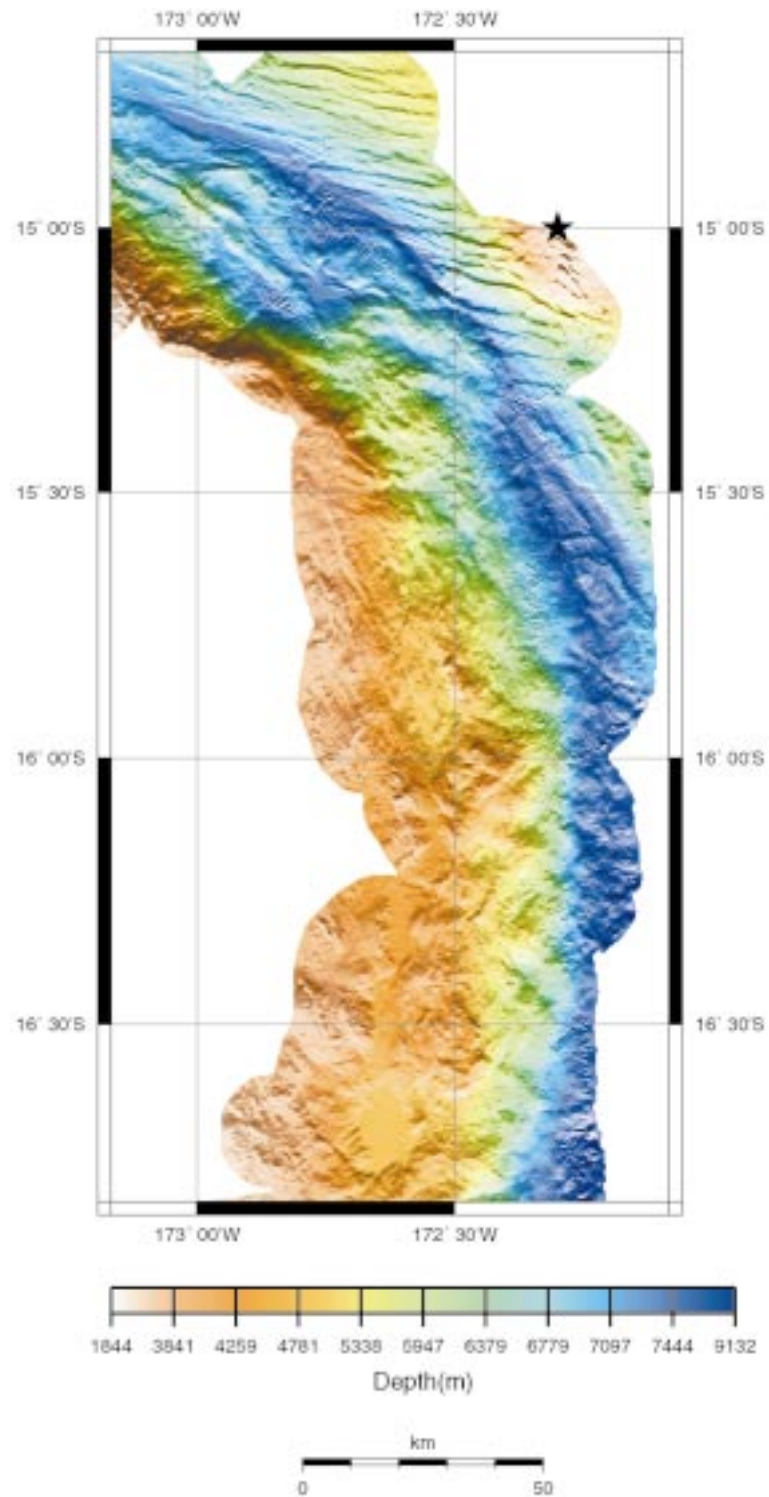
Figure 8. Histogram equalized, shaded relief bathymetric map of the northern forearc and westward bend in the Tonga Trench, created from a 200-m Sea Beam 2000 grid (Boomerang 8). Summit of Machias seamount denoted by star. The bathymetry is illuminated at an azimuth of 0° using a shading magnitude of 0.4 to accentuate the abyssal hill fabric at the bend in the trench. Color change interval based on histogram equalization. Map projection is Mercator.

evidence provided by Billington (1980), and recent confirmation supplied by the earthquake distributions and source mechanism determinations of Millen and Hamburger (1998). A possible bathymetric expression of the plate tearing is evident at 15°–16 °S where the landward trench slope steepens significantly, the forearc narrows, and the trench axis is 'pinched' by the presence of Machias seamount (Profiles 5–11, Figure 5). Also striking are the WNW-trending lineaments on portions of the Pacific Plate shown in Figure 8. These can be traced at least as far south as 15°20′ W, southwest of Machias seamount. These lineations, first described in detail by Hill and Tiffin (1993) from GLORIA and SeaMARC II data, have been interpreted as hinge faults, exhibiting a combination of normal and shear motion (Isacks et al., 1969; Wright, 1992; Millen and Hamburger, 1998). However, between 14°50′ and 15°30′ S the lineations systematically trend 280°–285°, even as the trench axis changes trend by ∼60°. In this region where the Pacific Plate is subducting and the bending hinge is at a high angle to the lineations, the apparent throw of these features does not increase towards the trench. This evidence suggests that these features are related to abyssal hill topography on the plate. The WNW trend of these lineations is consistent with recent work suggesting that the seafloor east of the Tonga Trench preserves a fabric formed at a roughly east-west trending spreading center (e.g., Castillo and Hawkins, 1998). We therefore interpret these lineations to be older Pacific Plate structures that have been reactivated by hinge-faulting at the bend in the trench.

The strike-slip portion of the trench terminates near 15°10′ S, where it truncates the mid- and lower slopes of the trench. South of this point, the trench narrows, becomes asymmetrical with a steeper landward slope, and convergence rapidly becomes near normal to the trench axis as the trench assumes a more north-south azimuth (Profiles 12–15, Figure 5). There are large, elongate highs on the western trench-slope break, inferred to be bounded by normal faults (Map 1), and some evidence of trenchward tilting of fault blocks (Profiles 13–15; Figure 5). There are also broad canyons in the landward trench slope (for example at 16°35′ S, 16°50′ S) facilitating the mass wasting of material into the trench (Clift et al., 1998).

Map 2: Normal convergence and seamount collision

Map 2 shows a section of the forearc that is probably typical of the 'equilibrium' profile of the trench.

As the Louisville Ridge collision passed through this region from 5.5 to about 3.3 Ma, the morphology of the trench here presumably represents that typical of tectonic erosion. A new seamount collision is just developing as Capricorn seamount (Raitt et al., 1955) enters the trench. The trench shoals west of Capricorn (Figure 9), and there is evidence that some small blocks may have been transferred from the subducting plate to the upper plate (as at 18°38′ S, 172°47′ W). Lonsdale (1986) and Clift et al. (1998) have suggested that a small accretionary prism exists west of Capricorn, in contrast to the tectonic erosion that dominates most of the trench.

The trench axis here comprises a series of en echelon basins, developed as grabens in the subducting plate enter the trench. Locally, what is morphologically the trench axis is structurally the axis of a graben in the Pacific Plate, and the plate boundary is actually within the landward slope (Hilde, 1983; Bloomer and Fisher, 1985; Lonsdale, 1986). Sediment is clearly not transported great distances longitudinally in the trench, and the graben serve to trap and then subduct clastic material moving down the trench slopes.

One of the most obvious features of the forearc here is the network of canyons and channels cutting the upper and middle slopes (as at 18°30′ S, 18°57′ S, 19°30′ S, 20°10′ S). These move material from the eastern parts of the Tonga Platform to large mid-slope basins such as those centered at 19 °S, 173°25′ W. There are also smaller canyons (e.g., 18°38′ S, 172°47′ W, Figure 9) that move material to the lower slopes and trench, but it appears that most clastic material is trapped in mid-slope basins. One of the largest of these canyons (at 18°30′ S) extends across the northern end of the Tonga Platform to the Tofua Arc, providing a path for volcaniclastics from the modern arc to be redeposited on the trench slopes. The prominent linear form of some of these canyons (as at 18°57′ S) suggests that they may have exploited faults that cut the forearc at high angles to the trench. Such faults may have developed in response to uplift and fracturing of the forearc during subduction of the Louisville Ridge.

The landward trench slopes in this area are steep, with prominent structural highs in the middle and lower landward slopes (Figures 5 and 6, Profiles 16–23). These structural highs are easily identifiable in Map 2, and commonly define the trench slope break at about 4000 m water depth. Similar structural blocks are common in the outer forearc, and everywhere that they were sampled (generally on their steepest flanks)
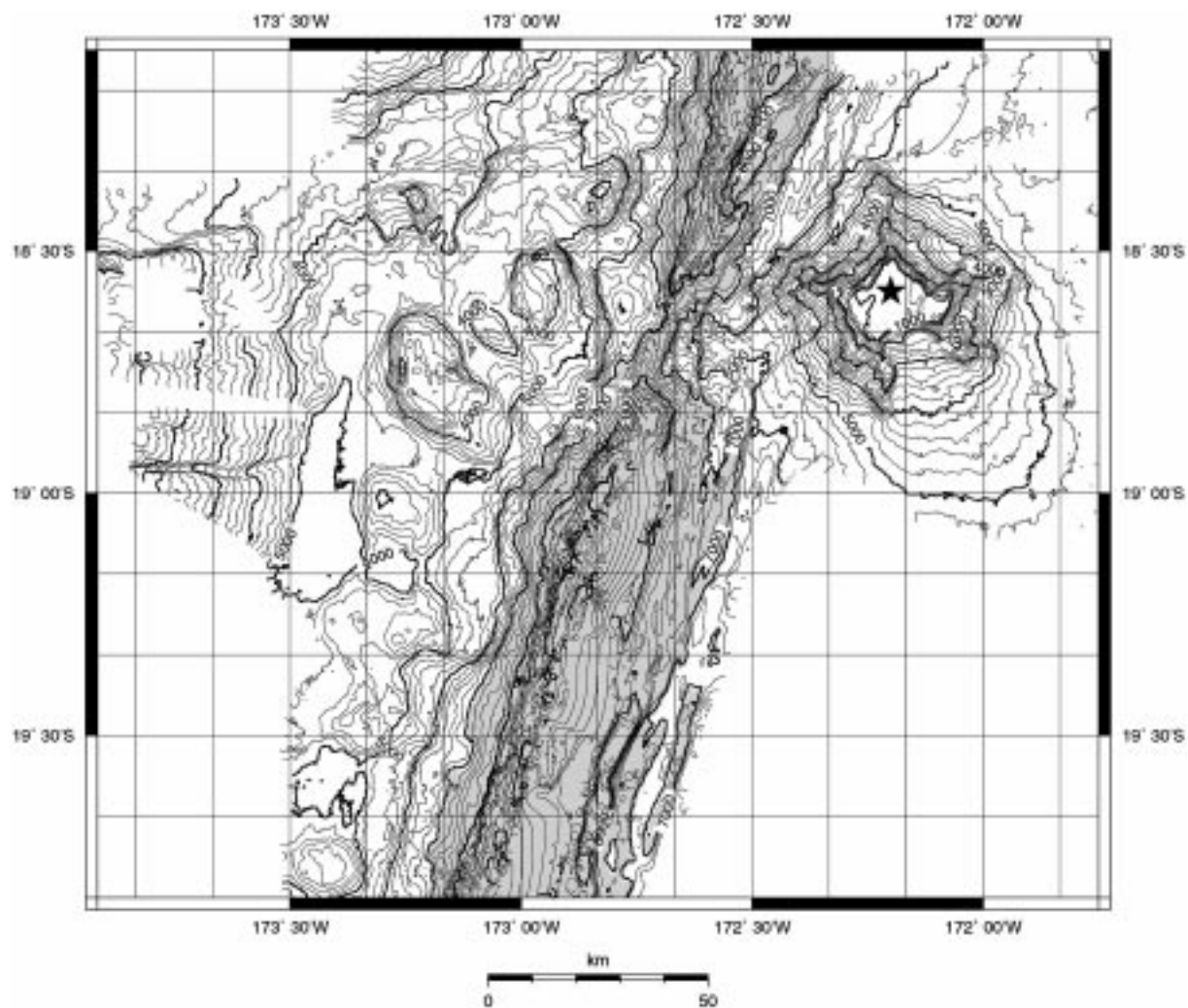
Figure 9. Bathymetric map (200-m contour interval) of the Tonga Trench and forearc, in the vicinity of Capricorn seamount (denoted by star). Shading indicates areas deeper than 7000 m. Note the distinct submarine canyon to the west of the trench at ~19 °S. Map was created from a 200-m Sea Beam 2000 grid (Boomerang 8), with portions of the trench axis filled in by Sea Beam data from Marathon 6. Map projection is Mercator.

the exposures comprise altered arc volcanic rocks and volcaniclastic sediments. Unlike the trench slope highs in the Izu-Mariana-Bonin system, most of which are serpentine diapirs (e.g., Fryer et al., 1985, 1990), the highs within the Tonga forearc appear to be fault blocks. Their shape in plan view is often irregular (Figure 9), which is not what would be expected of fault-bounded blocks, unless the faults are extremely low angle. However, there are some blocks that are asymmetrical (bounded by at least one steep, trench-parallel slope as at 20 °S, 173°30′ W and 18°23′ S, 172°50′ W), and thus appear to be fault-bounded. And there are some that retain a blocky form, bounded by trench-parallel slopes, but appear to have been partly dissected by canyons and channels (e.g., the large block from 19°15′ S, 173°15′ W to 19°30′ S, 173°20′ W). We suggest that most of the irregularly shaped highs along the slope break are fault-bounded blocks that have been dissected and degraded by erosion. The dredging results (Bloomer et al., 1996), in any case, found no evidence of serpentine diapirism as a contributing factor in the formation of these slope highs.

Map 3: Post-Louisville ridge collision geometry

Map 3 (at back) shows the widest cross-section of the arc and forearc (~90–100 km) from the East Lau Spreading Center in the west across the trench to the Pacific Plate. This area is just north of a large westward embayment in the forearc that has been attributed to collapse of the forearc in response to the subduction of the Louisville Ridge (Lonsdale, 1986; Pelletier and Dupont, 1990). Map 3 shows the northern edge of this embayment, presumably marking the point at which the forearc has re-equilibrated itself and re-established its critical taper, slightly more than 2 Ma after the passage of the Louisville Ridge.

In fact, this area shares many morphologic features in common with that in Map 2, which is also inferred to represent an 'equilibrium' profile for the forearc. The portion of the trench shown in Map 3 is somewhat deeper than to the north, but also has very steep lower slopes (in places > 10° at depths > 7000 m) and prominent structural highs on the midslopes and trench slope break. The trench axis again shows an en echelon structure, reflecting the subduction of the horsts and grabens of the offshore plate. Large canyons cut the forearc (Map 3, as at 22°30′ S, 21°55′ S, and 21°40′ S). The structural highs along the slope break, here at about 5000 m, are more clearly asymmetric with steep, trench-parallel eastern sides (Figure 10, for example at 21°50′ S, 174°10′ W and 22°25′ S, 174°10′ W), consistent with an origin as blocks bounded by normal faults. Dredges from some of these highs also yield altered volcanic rocks and volcaniclastic sediments. The less 'degraded' appearance of these blocks may be because they are younger, having developed after the more recent passage of the Louisville Ridge is this part of the trench.

Map 4: Horizon deep and Louisville Ridge collision zone

Map 4 shows the portion of the forearc most recently affected by the collision of the Louisville Ridge with the Tonga forearc. The current collision is occurring at 25°44′ S. The westward re-entrant in the trench beginning at 24°30′ S and extending northwards past 24°30′ S has been interpreted as an area where the forearc has collapsed and been eroded in the wake of the Louisville Ridge's passage (Lonsdale, 1986; Pelletier and Dupont, 1990; MacLeod and Lothian, 1996). The forearc was likely oversteepened as the Louisville Ridge was subducted and subsequently collapsed (Lonsdale, 1986; Pelletier and Dupont, 1990).

When the forearc re-established its critical taper, it is also likely that the erosion of the margin left the 50–80 km arcward shift of the trench axis relative to the pre-collision geometry (Figures 1; 3).

The deep re-entrant centered near 23°15′ S has a distinctly different geometry than the forearc to the north. The trench axis is more continuous, and deeper than to the north, because the westward retreat of the forearc has exposed a deeper part of the bending Pacific Plate (Map 4). The mean gradient of the seaward slope here is greater (Lonsdale, 1986) because the dip of the Pacific Plate increases with depth to an average of 15° (Billington, 1980). Although the upper slopes of the landward plate are steep, the overall gradient of the landward slope is gentler and more continuous than to the north (Figure 11; Figure 6, Profiles 27–29). The landward slope lacks the fault-bounded structural highs characteristic of the forearc to the north, and does not have a well-defined trench-slope break. While there are some small canyons and channels in the forearc, there are few of the very large canyons common in the forearc north of 23 °S. These morphologic differences are consistent with the hypothesis that this part of the forearc has recently collapsed and undergone substantial erosion at its base, after oversteepening by subduction of the Louisville Ridge. The collapse is recent enough that the large canyons and clearly defined normal faults that are part of the 'steady-state' subduction erosion geometry have not yet developed.

This re-entrant includes *the deepest spot in the entire southern hemisphere*, Horizon Deep, centered at about 23°15′ S in the trench axis. Fisher (1954) reported a bomb sounding from Horizon Deep of 10,633 m ± 27 m, corrected. The maximum depth in the deep has been estimated to be at least 10,800 ± 2 m, corrected, based on the interpretation of persistent flank echos in 12-kHz echo-sounder profiles (Fisher, 1954, 1974). Lonsdale (1986) reported a depth of 10,866 m, corrected, from Horizon Deep (assuming a sound velocity of 1500 m/s), confirming the estimate of Fisher (1954). The error on the 10,866 m depth must be greater than ± 55 m, based on the 0.5% accuracy assumed for Sea Beam center-beam depths in optimal conditions. The deepest, corrected, center-beam sounding on Sea Beam 2000 swaths during Boomerang 8 was 10,577 m at 23°13.60′ S, 174°43.54′ W, which is ~1.5 km north of Lonsdale's (1986) sounding and ~3 km north of Fisher's (1974) profiles. This depth was corrected based also on a sound velocity of 1500 m s^{-1} from an XBT cast made
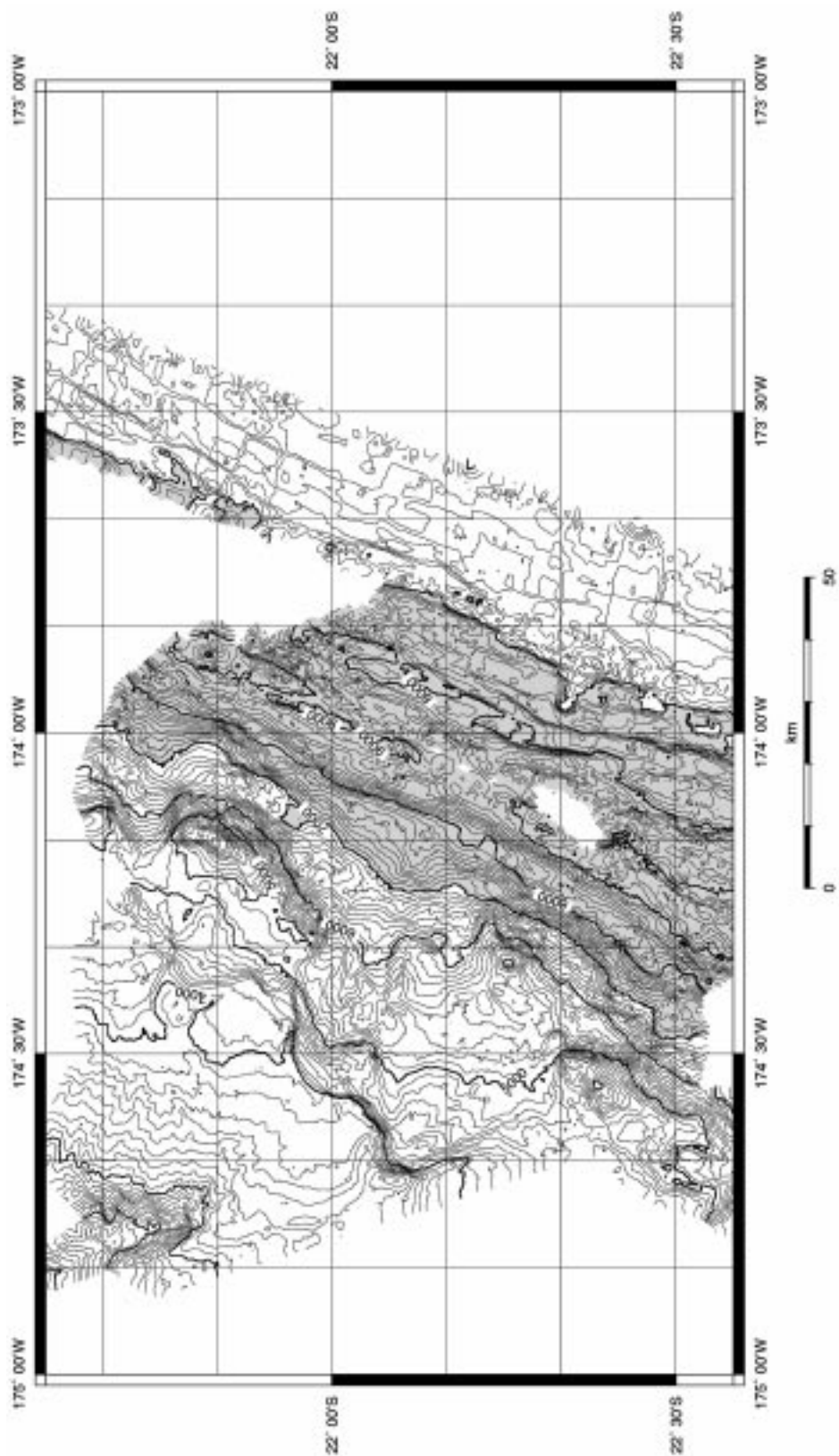
Figure 10. Bathymetric map (200-m contour interval) of the Tonga Trench and forearc, centered at 22 °S, as well as a portion of the Pacific plate. Shading indicates areas deeper than 7000 m. Map was created from a 200-m Sea Beam 2000 grid (Boomerang 8 and Westward 12). Map projection is Mercator.
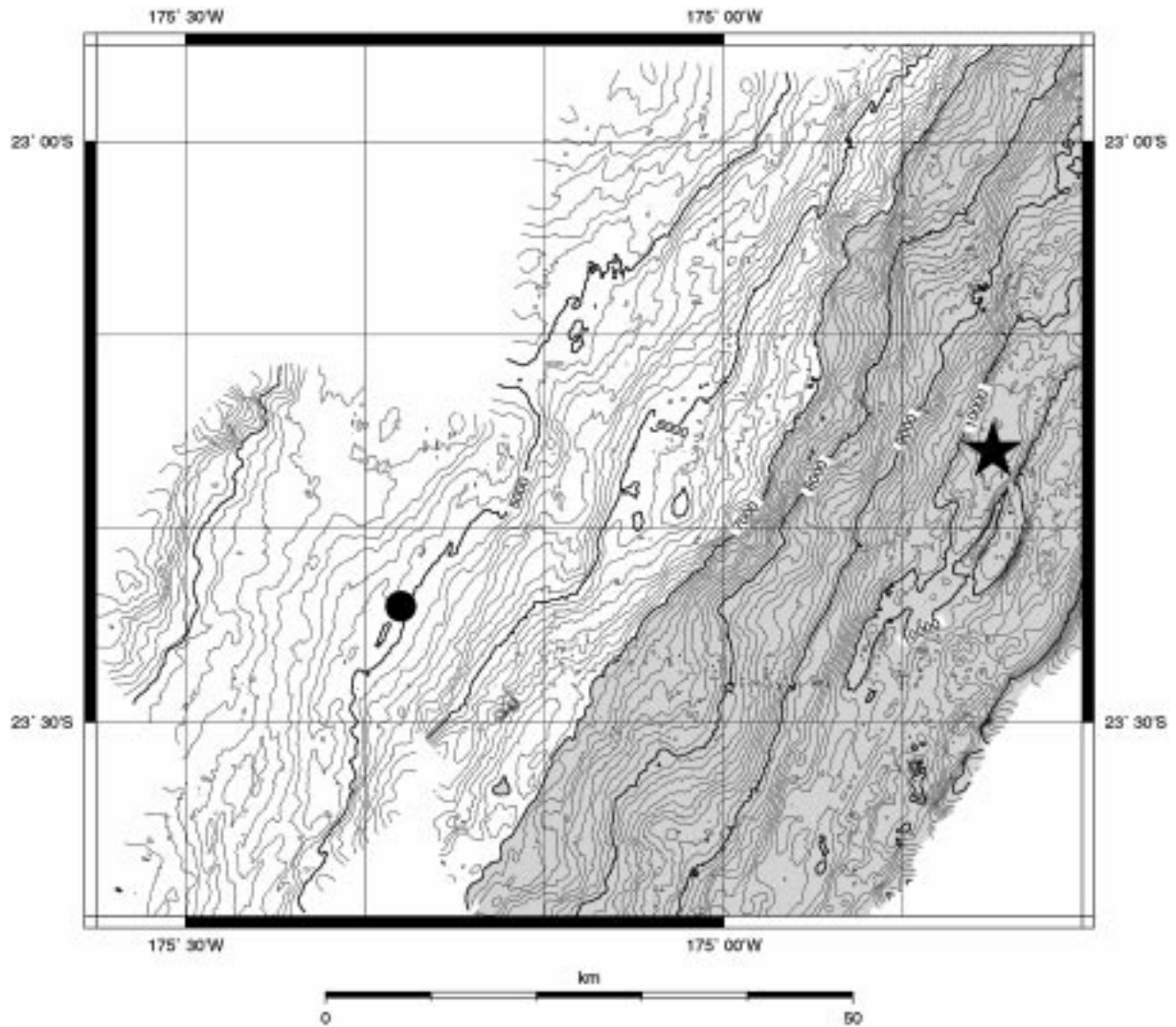
Figure 11. Bathymetric map (200-m contour interval) of the Tonga Trench in the vicinity of Horizon Deep (denoted by the star), deepest spot in the Southern Hemisphere. ODP Site 841 denoted by the circle. Shading indicates areas deeper than 7000 m. Map was created from a 200-m Sea Beam 2000 grid (Boomerang 8). Map projection is Mercator.

the day of the survey; the error on the sounding must again be greater than ± 55 m.

Collision and subduction of the Louisville Ridge at 26 °S has had a significant effect on the morphology of the forearc (cf., Gnibdenko et al., 1985; Lonsdale, 1986; Ballance et al, 1989; Pelletier and Dupont, 1990; MacLeod, 1994). The forearc has been uplifted and oversteepened with a substantial amount of normal faulting (e.g., Profile 30 in Figure 6 and Figure 12 particularly at ∼26 °S, 175°55′ W and 25°50′ S, 175°30′ W). Both trench parallel faults and faults at a high-angle to the trench (as marked by slopes or channels like that at 25°50′ S, 176°20′ W) are common.

The trench shoals as the seamounts of the Louisville Ridge are subducted, and there is morphologic and compositional evidence for the transfer of Cretaceous seamount material to the landward slopes of the trench (Map 4, small high at 25°45′ S, 175°18′ W; Balance et al., 1989). This deformation of the forearc due to seamount subduction is distinct from the background, 'steady-state' erosion, which is characterized by large-scale subsidence of the entire forearc and a gradual regional tilt towards the trench axis (MacLeod, 1994; Clift and MacLeod, 1999).
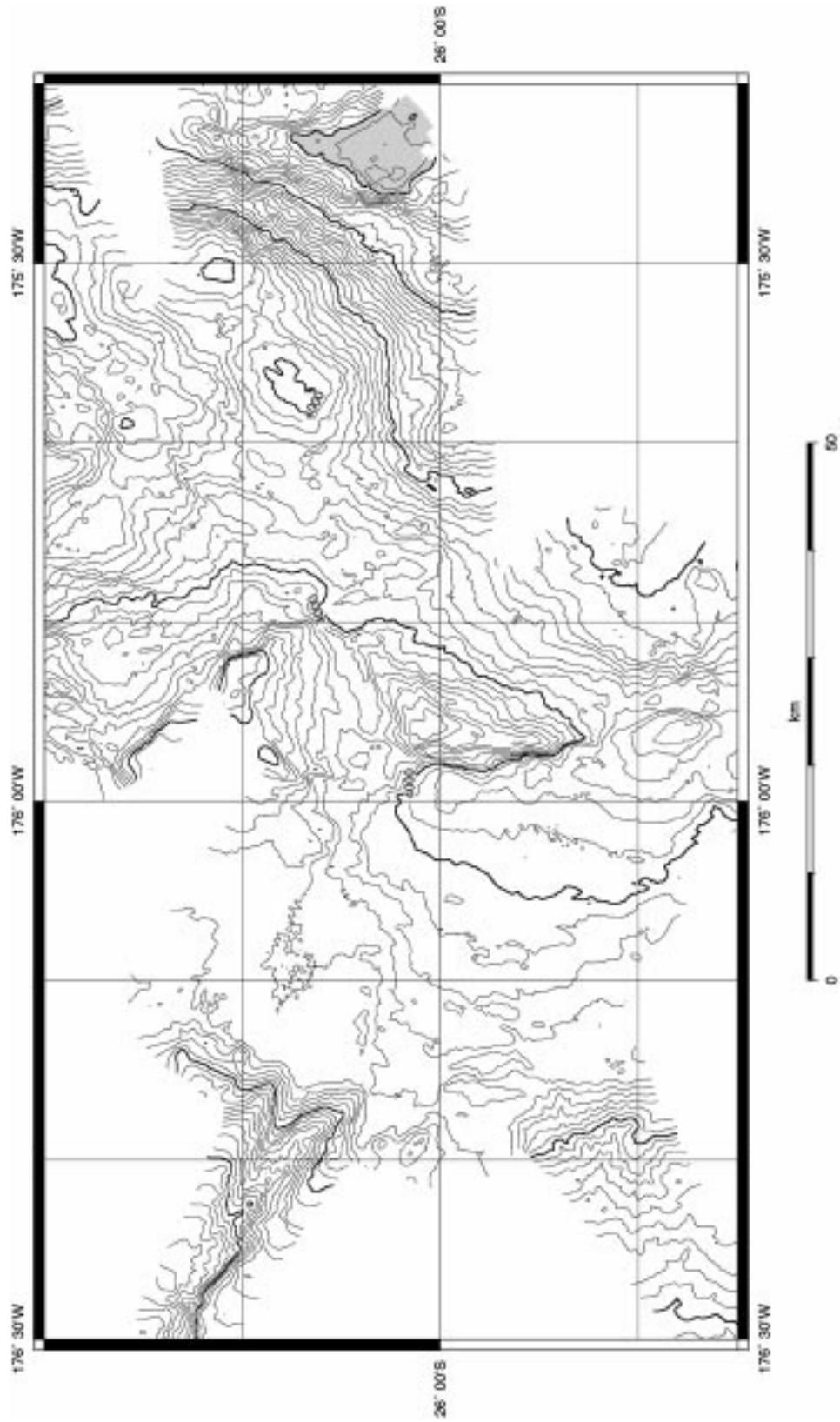
Figure 12. Bathymetric map (100-m contour interval) of the Tonga forearc, centered at 26 °S, just north of the Louisville Ridge collision with the trench. Shading indicates areas deeper than 7000 m. Map was created from a 200-m Sea Beam 2000 grid (Boomerang 8). Map projection is Mercator.

508

Conclusion

This new compilation of bathymetry documents changes in the morphologic characteristics of the Tonga Trench and forearc in response to changes in plate convergence directions and to the subduction of the seamounts of the Louisville Ridge. The Tonga Trench and forearc are dominated by abundant normal faulting, and typically have numerous canyons that allow substantial volumes of material to move from the Tonga platform to middle and lower slope basins. The central forearc, which is inferred to be undergoing 'steady-state' subduction erosion, is dominated the most by these features, as evidenced by the many large, trench-parallel scarps, most of which must have accommodated large-scale subsidence of the forearc and a gradual, regional tilt of fault blocks toward the trench axis. The southern forearc and trench show a different morphology and are strongly influenced by a spatially restricted and accelerated process of erosion resulting from the recent subduction of the Louisville Ridge. The causes and relative contributions of these two modes of tectonic erosion can best be determined in concert with drilling. Such drilling could constrain the timing of forearc subsidence from the litho- and biostratigraphy of the upper Eocene to Recent sediments overlying the basement (e.g., Clift, 1994). Borehole data could also help determine the timing and orientation of tectonic tilting of the forearc via sedimentary bedding attitudes in cores, and on Formation MicroScanner borehole logging images (e.g., MacLeod et al., 1992); and could be combined with seismostratigraphic models of the forearc platform (e.g., Tappin, 1994).

The process of tectonic erosion is still poorly understood, not least because it involves absence of the evidence, and is therefore difficult to document. Nevertheless, it is of vital importance as an important mechanism for delivering terrestrial material into the mantle (at a rate estimated to be comparable to the flux of juvenile igneous material returned to the Earth's crust; von Huene and Scholl, 1991). Several studies have shown that massive subsidence of forearcs is a fundamental consequence of tectonic erosion (e.g., in Japan and Chile: von Huene et al., 1988; von Huene and Culotta, 1989; von Huene and Lallemand, 1990). For Tonga, too, wholesale foundering of the forearc has occurred, with at least 5.4 km of subsidence recorded since the late Eocene at Site 841 (Clift, 1994). Clift and MacLeod (1999) have estimated that approximately 135 km of material has been eroded from the Tonga forearc since the Eocene.

Appendix

The bathymetry grids from which the large regional and detailed page-size maps were created are available on the World Wide Web at http://capnhook.geo.orst.edu/tonga/. The grids are binary, Unix-compressed, GMT-style grid files. Also available are the original postscript files of the maps, color 3-D visualizations of many of the smaller bathymetric grids, and a version of this manuscript with all figures in color at http://dusk.geo.orst.edu/tonga.

References

Ballance, P.F., Scholl, D.W., Vallier, T.L., Stevenson, A.J., Ryan, H. and Herzer, R.H., 1989, Subduction of a Late Cretaceous Seamount of the Louisville Ridge at the Tonga Trench: A Model of Normal and Accelerated Tectonic Erosion, *Tectonics* **8**: 953–962.

Beiersdorf, H. and von Stackelberg, U., 1990. Geoscientific Studies of the Manihiki Plateau and the Lau Basin, Southwestern Pacific - SO 67 (in German), *Jahresbericht für den Förderbereich Meeresgeowissenschaften*, 1990, 67–70.

Bevis, M., Taylor, F.W., Schultz, B.E., Recy, J., Isacks, B.L., Helu, S., Singh, R., Kendrick, E., Stowell, J., Taylor, B. and Calmant, S., 1995, Geodetic Observations of Very Rapid Convergence and Back-arc Extension at the Tonga Arc, *Nature* **374**: 249–251.

Billington, S., 1990, The Morphology and Tectonics of the Subducted Lithosphere in the Tonga-Fiji-Kermadec Region from Seismicity and Focal Mechanism Solutions, Ph.D. Thesis, Cornell University, Ithaca, New York.

Bloomer, S.H. and Fisher R.L., 1987, Petrology and Geochemistry of Igneous Rocks from the Tonga Trench: Implications for its Structure. *J. Geology* **95**: 469–495.

Bloomer, S.H. and Wright, D.J., 1996, *Summary of Site Survey Cruise Results, Boomerang Leg 08, in Support of Proposal 451, Ocean Drilling in the Tonga Forearc: Subduction Geodynamics, Arc Evolution, and Deformation Processes at a Non-Accretionary Convergent Margin*, Ocean Drilling Program Site Survey Data Bank, Palisades, New York.

Bloomer, S.H., Wright, D.J., and Boomerang Leg 8 Shipboard Scientific Party, 1996, Geology of the Tonga Forearc: A supra-subduction zone ophiolite, *Eos Trans. AGU* **77**: F325.

Bloomer, S.H., Ewart, A., Bryan, W. and Hergt, J., 1994, Geochemistry and Origin of Igneous Rocks from the Outer Tonga Forearc, in J. Hawkins, Parson, L., Allan, J. et al. (eds) *Proc. ODP, Sci. Results, 135*, Ocean Drilling Program, College Station, Texas, 625–646.

Brocher, T.M., 1985, On the Formation of the Vitiaz Trench Lineament and North Fiji Basin, in Brocher, T.M. (ed.), *Investigations of the Northern Melanesian Borderland*, Circum-Pacific Council for Energy and Mineral Resources Earth Science Series 3, Houston, Texas, 13–33.

Caress, D.W. and Chayes, D.N., 1995, New software for processing sidescan data from sidescan-capable multibeam sonars, *Proc. IEEE Oceans 95 Conference,* 997–1000.

Caress, D.W. and Chayes, D.N., 1996, Improved processing of hydrosweep DS multibeam data on the R/V *Maurice Ewing*, *Mar. Geophys. Res.* **18**: 631–650.

Caress, D.W., Spitzak, S.E. and Chayes, D.N., 1996, Software for multibeam sonars, *Sea Technol.* **37**: 54–57.

Castillo, P.R. and Hawkins, J.W., 1998, The composition of the subducting oceanic lithosphere mainly responsible for the chemical and isotopic variations of the Tonga-Kermadec Arc Lavas? *Eos, Trans. AGU* **79**: F397.

Clague, D.A. and Jarrard, R.D., 1973, Tertiary plate motion deduced from the Hawaiian-Emperor seamount chain, *Geol. Soc. Am. Bull.* **84**: 1135–1154.

Clift, P.D., 1994, Controls on the sedimentary and subsidence history of an active plate margin: an example from the Tonga Arc, Southwest Pacific, in J. Hawkins, Parson, L., Allan, J. et al. (eds), *Proc. ODP, Sci. Results, 135*, Ocean Drilling Program, College Station, Texas, 173–188.

Clift, P.D. and MacLeod, C.J., 1999, Slow rates of subduction erosion estimated from subsidence and tilting of the Tonga Forearc, *Geology* **27**: 411–414.

Clift, P.D., MacLeod, C.J., Tappin, D.R., Wright, D.J. and Bloomer, S.H., 1998, Tectonic controls on sedimentation in the Tonga Trench and Forearc, SW Pacific, *Geol. Soc. Am. Bull.* **110**: 483–496.

Cochran, J.R., Fornari, D.J., Malinverno, A., Wang, X. and Goff, J.A., 1992, Systematic variation of summit and flank morphology within a ridge segment: East Pacific Rise, 7 °S–9 °S, *Eos, Trans. AGU* **73**: 313.

DeMets, C., Gordon, R.G., Argus, D.F. and Stein, S., 1990, Current plate motions, *Geophys. J. Int.* **101**: 425–478.

Dupont, J. and Herzer, R.H., 1985, Effect of subduction of the Louisville Ridge on the structure and morphology of the Tonga Arc, in Scholl, D.W. and Vallier, T.L. (eds), *Geology and Offshore Resources of Pacific Island arcs-Tonga Region,* Circum-Pacific Council for Energy and Resources, *Earth Science Series* **2**: 323–332.

Falloon, T., Bloomer, S.H., Crawford, S.H. and Wright, D.J., submitted, Geochemistry of dredged boninite series volcanics from the Tongan Forearc: implications for the nature of early arc volcanism, *Earth Planet. Sci. Lett.*

Fisher, R.L., 1954, On the sounding of trenches, *Deep-Sea Res.* **2**: 48–58.

Fisher, R.L., 1974, Pacific-type continental margins, in C.A. Burk and C.L. Drake (eds), *The Geology of Continental Margins*, Springer-Verlag, New York, 25–41.

Fisher, R.L. and Engel, C.G., 1969, Ultramafic and basaltic rocks dredged from the nearshore flank of the Tonga Trench. *Geol. Soc. Amer. Bull.* **80**: 1373–1378.

Fryer, P., Ambos, E.L. and Hussong, D.M., 1985. Origin and emplacement of Mariana Forearc Seamounts, *Geology* **13**: 774–777.

Fryer, P., Pearce, J.A., Stokking, L.B., et al. (eds), 1990, *Proc. ODP, Sci. Results, 135*, Ocean Drilling Program, College Station, Texas, 1092 pp.

Gnibidenko, H.S., Anosov, G.I., Argentov, V.V. and Pushchin, I.K., 1985, Tectonics of the Tonga-Kermadec trench and Ozbourn Seamount, *Tectonophysics* **112**: 357–383.

Hamburger, M.W. and Isacks, B.L., 1988, Diffuse back-arc formation in the southwestern pacific, *Nature* **332**: 599–604.

Hawkins, J.W., 1974, Geology of the Lau Basin, a Marginal Sea Behind the Tonga Arc, in C.A. Burk and C.L. Drake (eds), *The Geology of Continental Margins*, Springer-Verlag, New York, 505–524.

Hawkins, J.W., 1986, 'Black smoker' Vent Chimneys, Lau Basin, *Eos, Trans. AGU* **67**: 430–431.

Hawkins, J.W., 1995, Evolution of the Lau Basin–Insights from ODP Leg 135, in B. Taylor and J. Natland (eds), *Active Margins and Marginal Basins of the Western Pacific*, American Geophysical Union, Washington, D.C., 125–173.

Hawkins, J.W., Bloomer, S.H., Evans, C.A. and Melchior, J.T., 1984, Evolution of intra-oceanic arc-trench systems, *Tectonophysics* **102**: 175–205.

Hawkins, J.W. and Natland, J.H., 1975, Nephelinites and basanites of the samoan linear volcanic chain: their possible tectonic significance, *Earth Planet. Sci. Lett.* **24**: 427–439.

Hawkins, J.W., Parson, L.M. and Allan, J.F., 1994, Introduction to the scientific results of leg 135: Lau Basin-Tonga Ridge drilling transect, in J. Hawkins, L. Parson, J. Allan, et al. (eds), *Proc. ODP, Sci. Results, 135*, Ocean Drilling Program, College Station, Texas, 3–5.

Hilde, T.W.C., 1983, Sediment subduction versus accretion around the Pacific, *Tectonophysics* **99**: 381–397.

Hill, P.J. and Tiffin, D.L., 1993, Geology, sediment patterns, and widespread deformation on the sea floor off western samoa revealed by wide-swath imagery, *Geo-Marine Lett.* **13**: 116–125.

Hussong, D. and Uyeda S., 1981, Tectonic Processes and the History of the Mariana Arc: A Synthesis of the Results of Deep Sea Drilling Project Leg 60, in D.M. Hussong, S. Uyeda, et al. (eds), *Initial Reports of the Deep Sea Drilling Project*, *31*, U.S. Govt. Printing Office, Washington D.C., 909–929.

Isacks, B.L., Oliver, J. and Sykes, L.R., 1968, Seismology and the new global tectonics, *J. Geophys. Res.* **73**: 5855–5899.

Isacks, B.L., Sykes, L.R. and Oliver, J., 1969, Focal mechanisms of deep and shallow earthquakes in the Tonga-Kermadec region and the tectonics of Island Arcs, *Geol. Soc. Am. Bull.* **80**: 1443–1470.

Keeton, J.A., Searle, R.C., Parsons, B., White, R.S., Murton, B.J., Parson, L.M., Peirce, C. and Sinha, M.C., 1997, Bathymetry of the Reykjanes Ridge, *Mar. Geophys. Res.* **19**: 55–64.

Kelman, M., 1998, Hydrothermal Alteration of a Supra-Subduction Zone Ophiolite Analog, Tonga, Southwest Pacific, Master's Thesis, Oregon State University, Corvallis, Oregon.

Kroenke, L.W., Jarvis, P.A. and Price, R.C., 1987, Morphology of the Fiji fracture zone: recent reorientation of plate boundaries in the vicinity of the north Fiji Basin, *Eos, Trans. AGU* **68**: 1445.

Lonsdale, P., 1986, A multibeam reconnaissance of the Tonga Trench axis and its intersection with the Louisville Guyot Chain, *Mar. Geophys. Res.* **8**: 295–327.

Lonsdale, P., 1988, Geography and history of the Louisville Hotspot chain in the Southwest Pacific, *J. Geophys. Res.* **93**: 3078–3104.

Macdonald, K.C., Fox, P.J., Carbotte, S., Eisen, M., Miller, S., Perram, L., Scheirer, D., Tighe, S. and Weiland, C., 1992, The East Pacific rise and its flanks, 8°–17 °N: history of segmentation, propagation and spreading direction based on SeaMARC II and sea beam studies, *Mar. Geophys. Res.* **14**: 299–334.

MacLeod, C.J., 1994, Structure of the outer Tonga Forearc at site 841, in J. Hawkins, Parson, L., Allan, J. et al. (eds), *Proc. ODP, Sci. Results, 135*, Ocean Drilling Program, College Station, Texas, 313–329.

MacLeod, C.J., 1996, Geodynamics of the Tonga subduction zone and Lau Backarc basin, *Eos Trans. AGU* **77**: F325.

MacLeod, C.J., Parson, L.M., Sager, W.W. and the ODP Leg 135 Scientific Party, 1992, Identification of Tectonic Rotations in Boreholes by the Integration of Core Information With Formation MicroScanner and Borehole Televiewer Images, in A. Hurst, C.M. Griffiths and P.F. Worthington (eds), *Geological Applications of Wireline Logs, Geological Society of London Special Publication, London* **65**: 235–246.

MacLeod, C.J., Wright, D.J., Bloomer, S.H. and Clift, P.D. (in preparation) Structure of the Tonga Forearc and Geodynamic Evolution of the Tonga-Lau Marginal Basin System.

Millen, D.M. and Hamburger, M.W., 1998, Seismological evidence for tearing of the pacific plate at the northern termination of the Tonga subduction zone, *Geology* **26**: 659–662.

Miller, S.P. and Capell, W.J., 1993, Multibeam sonars: families for multi-mission Vessels, *Sea Technol.* **34**: 10–15.

New Zealand Hydrographic Office, 1977, South Pacific Ocean, *New Zealand to Fiji and Samoa Islands*, Defense Mapping Agency Hydrographic Center, Washington, D.C., 1 map sheet, 1:3,500,000.

Olbertz, D., Wortel, M.J.R. and Hansen, U., 1997, Trench migration and subduction zone geometry, *Geophys. Res. Lett.* **24**: 221–224.

Parson, L.M. and Tiffin, D.L., 1993, Northern Lau Basin: backarc extension at the leading edge of the Indo-Australian plate, *Geo-Marine Lett.* **13**: 107–115.

Parson, L.M. and Hawkins, J.W., 1994. Two-stage ridge propagation and the geological history of the Lau Backarc basin, in J. Hawkins, L. Parson, J. Allan et al. (eds), *Proc. ODP, Sci. Results, 135*, Ocean Drilling Program, College Station, Texas, 819–828.

Pelletier, B. and Dupont, J., 1990, Effets de la subduction de la ride de Louisville sur l'arc des Tonga-Kermadec, *Ocean. Acta* **10**: 57–76.

Pelletier, B. and Louat, R., 1989, Mouvements relatifs des plaques dan le sud-ouest pacifique, *C.R. Acad. Sci.* **308**: 123–130.

Pontoise, B., Pelletier, B., Aubouin, J., Baudry, N., Blanchet, R., Butscher, J., Chotin, P., Diament, M., Dupont, M., Eissen, J., Ferrière, J., Herzer, R., Lapouille, A., Louat, R., d'Ozouville, L., Soakai, S. and Stevenson, A., 1986, Subduction of the Louisville Ridge along the Tonga Trench: preliminary results of SEAPSO campaign (Leg V), *Compte Rendu de l'Academie des Sciences, Série II* **10**: 911–918.

Purdy, G.M., Sempéré, J.-C., Schouten, H., Dubois, D. L. and Goldsmith, R., 1990, Bathymetry of the mid-atlantic ridge, 24°–31 °N: a map series, *Mar. Geophys. Res.* **12**: 247–252.

Raitt, R.W., Fisher, R.L. and Mason, R.G., 1955, Tonga Trench, *Geol. Soc. Amer. Spec. Paper* **62**: 237–254.

Sager, W.W., MacLeod, C.J. and Abrahamsen, N., 1994, Paleomagnetic Constraints on Tonga Arc Tectonic Rotation from Sediments Drilled at Sites 840 and 841, in J. Hawkins, L. Parson, J. Allan et al. (eds), *Proc. ODP, Sci. Results, 135*, Ocean Drilling Program, College Station, Texas, 763–786.

Sandwell, D.T., 1987, Biharmonic spline interpolation of GEOS-3 and seasat altimeter data, *Geophys. Res. Lett.* **14**, 139–142.

Scheirer, D.S., Macdonald, K.C., Forsyth, D.W., Miller, S.P., Wright, D.J., Cormier, M.-H., and Weiland, C.M., 1996, A map series of the Southern East Pacific rise and its flanks, 15 °S to 19 °S, *Mar. Geophys. Res.* **18**: 1–12.

Smith, G.P., Wiens, D.A., Dorman, L.M., Webb, S.C. and Fischer, K.M., 1998, Azimuthal anistropy beneath the Lau Basin: observations of shear wave splitting from local earthquakes at ocean bottom seismometers, *Eos Trans. AGU* **79**: F637.

Tappin, D.R., 1994, The Tonga Frontal-arc basin, in P.F. Ballance (eds.) *South Pacific Sedimentary Basins*, Elsevier, Amsterdam, 157–176.

Tappin, D.R., Bruns, T.R. and Geist, E.L., 1994a, Rifting of the Tonga/Lau Ridge and Formation of the Lau backarc basin: evidence from site 840 on the Tonga Ridge, in J. Hawkins, L. Parson, J. Allan et al. (eds), *Proc. ODP, Sci. Results, 135*, Ocean Drilling Program, College Station, Texas, 367–372.

Tappin, D.R., Herzer, R.H. and Stevenson, A.J., 1994b, Structure and Stratigraphy of the Southern Tonga Ridge, 22°–26° South, in R.H. Herzer, P.F. Ballance and A.J. Stevenson (eds), *Geology and Resources of Island Arcs - Tonga-Lau-Fiji Region,* SOPAC Technical Bulletin **8**: 81–100.

Taylor, B., Zellmer, K., Martinez, F. and Goodliffe, A., Sea-floor spreading in the Lau Back-arc basin, 1996, *Earth Planet. Sci. Lett.*, **144**: 35–40.

Taylor, B., Coffin, M., Dietrich, W., Dixon, T., Driscoll, N., Karner, G., Klemperer, S., Kohlstedt, D., Moore, C., Nittrouer, C., Plank, T., Sawyer, D., Stern, R., Stolper, E., Underwood, M. and Wiens, D., 1998, Program Focuses Attention on Continental Margins, *Eos, Trans. AGU* **79**: 137–142.

Vallier, T.L., O'Connor, R.M., Scholl, D.W., Stevenson, A.J. and Quinterno, P.J., 1985, Petrology of rocks dredged from the landward slope of the Tonga Trench: implications for middle miocene volcanism and subsidence of the Tonga Ridge, in D.W. Scholl, and T. L. Vallier (eds), *Geology and Offshore Resources of Pacific Island arcs-Tonga Region,* Circum-Pacific Council for Energy and Resources, Earth Science Series **2**: 109–120.

von Huene, R. and Culotta, R., 1989, Tectonic erosion at the front of the Japan trench convergent margin, *Tectonophysics* **160**: 75–90.

von Huene, R. and Lallemand, S., 1990, Tectonic erosion along the Japan and Peru convergent margins, *Geol. Soc. Am. Bull.* **102**: 704–720.

von Huene, R. and Scholl, D.W., 1991, Observations at convergent margins concerning sediment subduction, subduction erosion, and the growth of continental crust, *Rev. Geophys.* **29**: 279–316.

von Huene, R., Suess, E. and the ODP Leg 112 Scientific Party, 1988, Ocean drilling program leg 112, Peru continental margin: Part 1, Tectonic history. *Geology* **16**: 934–938.

von Rad, U., Riech, V., Wissmann, G., Stevenson, A. J., Morton, J.L. and Sinha, M.C., 1990, Seafloor reflectivity, sediment distribution, and magnetic anomalies of the Lau Basin (SW Pacific, SO35/48 cruises), *Marine Mining* **9**: 157–181.

von Stackelberg, U. and von Rad, U., 1990, Geological evolution and hydrothermal activity in the Lau and North Fiji Basins, Southwest Pacific Ocean: results of SONNE Cruise SO-35, *Geologisches Jahrbuch. Reihe D: Mineralogie, Petrographie, Geochemie, Lagerstaettenkunde* **92**: 1–660.

Watts, A.B., Weissel, J.K., Duncan, R.A. and Larson, R.L., 1988, Origin of the Louisville Ridge and its relationship to the Eltanin fracture zone, *J. Geophys. Res.* **93**: 3051–3077.

Wessel, P. and Smith, W.H.F., 1995, New version of the generic mapping tools released, *Eos, Trans. AGU* **76**: 329.

Wiedicke, M. and Collier, J., 1993, Morphology of the Valu Fa spreading ridge in the Southern Lau basin, *J. Geophys. Res.* **98**: 11,769-11,782.

Wiedicke, M. and Habler, W., 1993, Morphotectonic characteristics of a propagating spreading system in the Northern Lau Basin, *J. Geophys. Res.* **98**: 11,783–11,797.

Wright, D.J., 1992, Convergence and strike-slip motion at the northern terminus of the Tonga Trench, Southwest Pacific, in R.A. Geyer (ed.), *CRC Handbook of Geophysical Exploration at Sea*, CRC Press, Boca Raton, Florida, 35–79.